UNCLASSIFIED

NRL Report 7171

The Possibility of Electromagnetic Wave Ducting in the Ionosphere

S. J. STEPHANAKIS, W. W. BALWANZ, W. S. AMENT, AND W. R. FAUST

Applied Physics Branch
Applications Research Division

November 6, 1970

NAVAL RESEARCH LABORATORY
Washington, D.C.

This document has been approved for public release and sale; its distribution is unlimited.

UNCLASSIFIED

CONTENTS

ABSTRACT

The refractive index of the ionosphere varies with altitude, providing optimum wave curvature for around-the-world propagation. The variation also provides ducts which tend to focus waves into this optimum curvature.

Simple calculations using published ionospheric properties are used to demonstrate the wave curvature and the duct structure. The duct altitude varies between 90 and 300 km depending on the frequencies used and the diurnal variations of the ionosphere. Signal loss varies widely, providing around-the-world propagation with less than a 5-dB loss per earth traverse in some of the duct configurations.

Methods of coupling into the ducts are assumed based on reports by other investigators. Signal scatter, which provides one method for coupling into and out of the duct, adds to the calculated signal loss from electron collisions.

PROBLEM STATUS

This is a final report on the application of this study to the ionosphere; the study of inhomogeneous plasmas is continuing.

AUTHORIZATION

NRL Problem R07-07
Project RF 17-344-401-4503

Manuscript submitted July 31, 1970.

UNCLASSIFIED

THE POSSIBILITY OF ELECTROMAGNETIC WAVE DUCTING IN THE IONOSPHERE*

LIST OF SYMBOLS

a	earth's radius
e	electronic charge
$\bar{E}$	electric field
h	altitude
h_1	injection altitude
j	$\sqrt{-1}$
$\bar{J}$	electronic conduction current density
m	electronic mass
M	modified refractive index
M_1	modified refractive index at injection altitude
n	refractive index
N_e	electron density
P	pressure
r	range along earth's surface
T	temperature
$\bar{v}$	electronic velocity
α	attenuation coefficient
β	phase shift coefficient
ϵ_0	free-space permittivity
λ	wavelength
μ_0	free-space permeability
ν	total electron collision frequency
ν_{em}	electron-neutral collision frequency
ν_{ei}	electron-ion collision frequency
σ	complex conductivity
ϕ	angle subtended at the earth's center by the arc traversed
ψ_1	angle between the direction of propagation and the tangent to the earth's surface at injection altitude
ψ_{cr}	critical angle between the direction of propagation and the tangent to the earth's surface for wave confinement within the duct
ω	electromagnetic radian frequency
ω_p	plasma radian frequency

*Note: A brief synposis of this report was given orally under the same title at the 1970 Spring Meeting of URSI in Washington, D. C., on April 16, 1970.

INTRODUCTION

Background

The phenomenon of Round the World (RTW) propagation has intrigued scientists, and in particular experimentalists, since it was first reported more than 40 years ago by Quäck (1,2). Between 1927 and 1930 a number of papers appeared on the subject (3-5). These early investigators found that the delay time between the transmitted signal and the first echo signal was about 138 msec and that the twilight hours seemed to be most conducive to such observations.

More extensive investigations of the phenomenon were carried out during World War II in Germany and Denmark by von Schmidt and Hess and were described in detail by Hess (6) in 1948. By this time it was shown that the attenuation suffered by the signal per revolution around the earth could be very small (i.e., as small as 5 dB). Furthermore, it was pointed out that the distortion suffered by such circulating signals was much less severe than observed direct-signal distortion and in sharp contrast with the destructive phase interference and dispersive effects suffered by multihop signals.

In 1958 Isted (7) reported on RTW signals at 37 MHz transmitted from Gibraltar and received at Hanningfield, Essex, England, and on 20-MHz signals transmitted from the USSR Satellite 1957 Alpha and received at Great Baddow, England. Isted shows that RTW signals need not be restricted to frequencies below the normal F_2 MUF and suggests a tilted-layer model of injection and subsequent continuous scattering to the ground once the wave enters the circulating mode.

Al'pert (8) in his book published in Moscow in 1960 also has a brief discussion of RTW propagation and among other examples he shows data received at the Mirny Station in the Antarctica transmitted at 20 MHz by the Sputnik I. Signal echoes from the antipodal points are easily discernible on the reproduced record, and Al'pert mentions that such echoes were observed in four successive orbits. He and Whale (9) tend to believe that these signals are directly related to RTW propagation.

In 1963 Fenwick (10) reported on experimental and theoretical work carried out at Stanford University during 1961 and 1962. He ultimately reached the conclusion that the dominant RTW propagation mode ". . . is a low-angle earth-ionosphere-earth hop mode, primarily in the sunlit hemisphere, plus an ionosphere-ionosphere tilt-mode in a portion of the dark hemisphere."

Whale (9) recently stated that at least as far as he is concerned the question is by no means resolved.

Purpose of the Report

The purpose of this report is to present a model for RTW propagation via ionospheric ducting based on an examination of ionospheric properties at altitudes between 90 and 300 km with particular emphasis on its refractive properties for a range of frequencies from 1 to 30 MHz. It is determined by the analysis of the resultant refractive index profiles that the ionosphere is capable of supporting trapped modes of propagation circumferencially around the earth and that such paths are low-attenuation paths consistent with the experimental observations mentioned above.

UNCLASSIFIED

THE IONOSPHERIC PARAMETERS

The parameters which can influence radio wave propagation through an ionized medium and which are properties of that medium are the charged-particle density, the interparticle collision frequency, and the magnetic field which may exist in the region.

For the electromagnetic frequencies considered here the influence of ions is minute and can be neglected when compared with the influence of the electrons. This is due to the slowness of response of the massive ions to the rapidly varying electromagnetic fields resulting in practically no energy being transferred from the field to the ions or vice-versa.

The magnetic field is also ignored in this presentation since the gyro frequency for the B field in the region of interest is at least an order of magnitude smaller than the lowest electromagnetic frequency used. This last assumption can be avoided by inclusion of the gyro frequency in the propagation equations. Such an inclusion, however, complicates the analysis considerably, and it is not felt that it will significantly alter the final results.

The electron collision frequency is several orders of magnitude smaller than the electromagnetic frequency. However, it must be pointed out that the collision frequency cannot be ignored since it plays the dominant role in the attenuation calculations.

The Electron Density

The electron density profiles used as the starting point for this calculation were obtained from an article by Wakai (11) in which he gives profiles obtained from the analysis of low-frequency ionograms (50-2000 kHz) at Boulder, Colorado, for 3 days and nights of quiet, moderate, and severe geomagnetic activity. These particular data were chosen because of the comprehensiveness of observations at a single site by a single investigator and because the profiles ranged over the times of day and altitudes of interest.

The quiet-twilight, quiet-nighttime, and moderate-twilight conditions are examined. Figures 1 and 2 show the electron density profiles for these cases as taken from Wakai's paper.

The Collision Frequency

The electron collision frequency ν is taken as the sum of the electron-neutral ν_{em} and the electron-ion ν_{ei} collision frequencies. These two frequencies are in turn calculated using relations from Ref. 12:

$$\nu_{em} = 3.5 \times 10^9 \, PT^{-1/2} \tag{1}$$

and

$$\nu_{ei} = \left[34 + 3.63 \, \ell n \left(T^{3/2} / N_e^{1/2}\right)\right] N_e / T^{3/2}, \tag{2}$$

where P is the total pressure in mm Hg, T is the electron temperature in °K, and N_e is the electron density in cm^{-3}. Pressure profiles (13) and temperature profiles (14) are also adapted from the existing literature.

In this semiempirical analysis, the diurnal and latitudinal variations of the electron temperature as well as its variation with the extent of magnetic disturbances have been ignored.

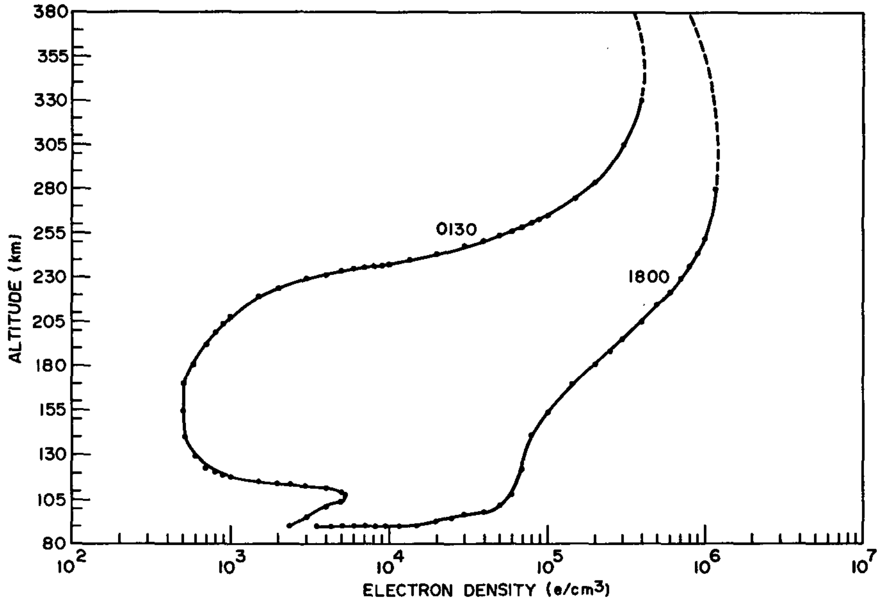

Fig. 1 - Electron density profiles for a magnetically quiet ionosphere taken at Boulder, Colorado, on Apr. 20-21, 1960

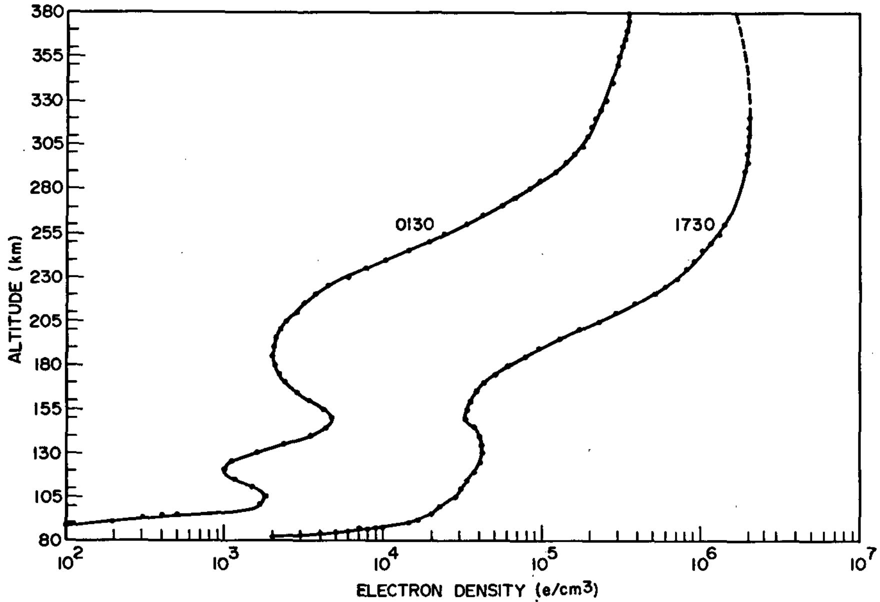

Fig. 2 - Electron density profiles for a moderately disturbed ionosphere taken at Boulder, Colorado, on Feb. 19-20, 1958

UNCLASSIFIED

The electron-neutral collision frequency used here does not include the effect of the dissociation of molecular oxygen into atomic oxygen. This effect was examined using the theoretical formulas of Banks (15) and the model atmosphere as given by Colegrove, et al. (16). It was found that the effect reaches maximum importance between a 100- and 200-km altitude. However, even in that region the electron-atom collision frequency was found to constitute less than 12% (at approximately 160 km) of the total collision frequency. This figure, it is felt, is within the tolerance of the experimentally obtained profiles and can thus be ignored.

The collision-frequency-vs-altitude curves obtained by the above procedure are shown in Figs. 3 and 4.

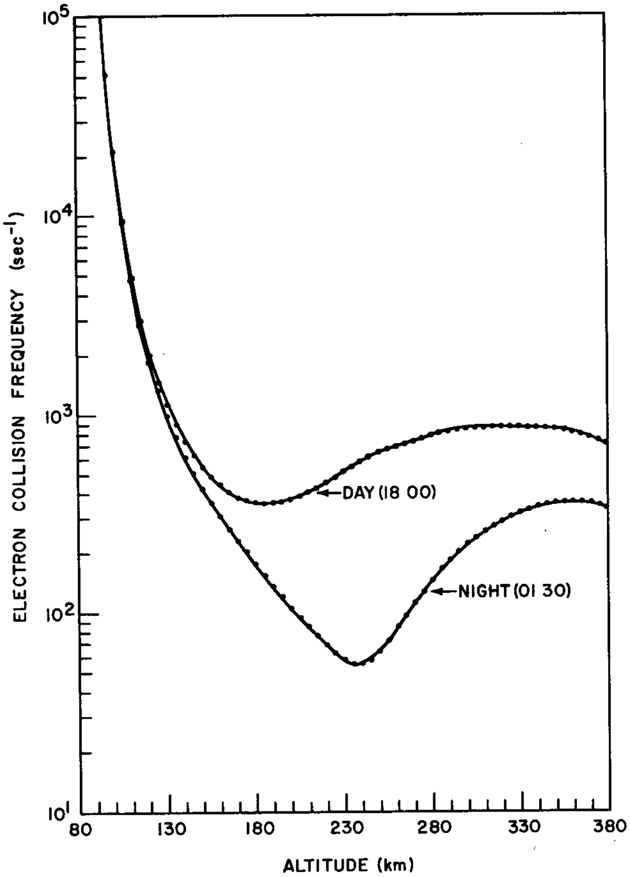

Fig. 3 - Collision frequency profiles for magnetically quiet ionosphere

THE PROPAGATION EQUATIONS

The assumption that the properties of the ionosphere (i.e., conductivity and permittivity) do not vary to any great extent over altitude increments of several wavelengths and several mean-free paths allows the propagation equations to be derived simply. The validity of this assumption is not easily demonstrable because measurements of any accuracy are not available which show the variation in the magnitude of these parameters over increments of meters or even hundreds of meters.

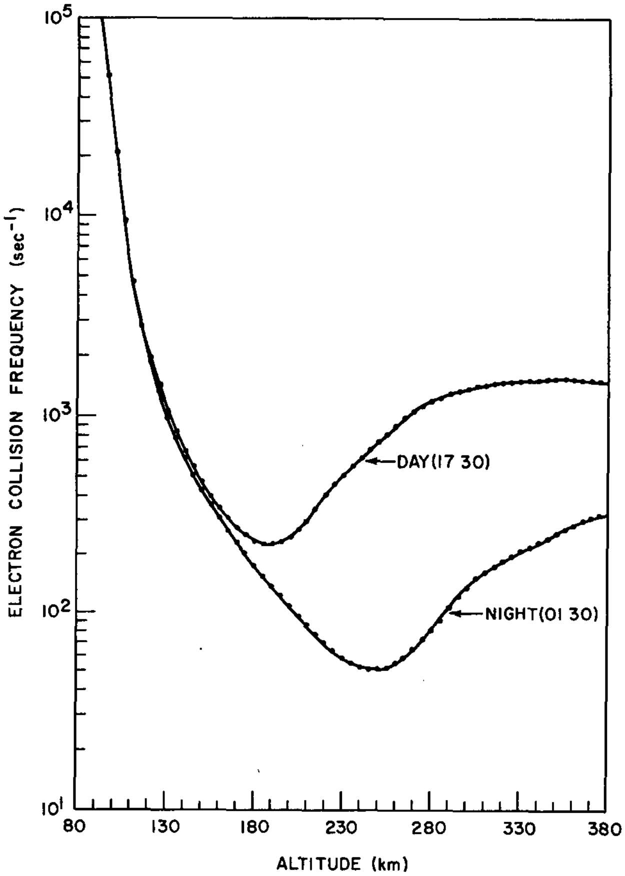

Fig. 4 - Collision frequency profiles for moderately disturbed ionosphere

Sinusoidal time variation of the electric field E and the electron velocity v, in the form $e^{j\omega t}$, and an electron collision frequency independent of velocity are assumed. The Lorentz equation

$$m \frac{d\bar{v}}{dt} + m\nu\bar{v} = e\bar{E}, \tag{3}$$

and Ohm's law for the conduction current density $\bar{J}$,

$$\bar{J} = N_e e\bar{v} = \sigma\bar{E}, \tag{4}$$

are used to obtain the plasma complex conductivity σ in terms of the electron density N_e, the collision frequency ν, the electromagnetic frequency ω, and the electronic charge and mass e and m, i.e.,

$$\sigma = \frac{N_e e^2}{m(\omega^2 + \nu^2)} (\nu - j\omega). \tag{5}$$

UNCLASSIFIED

Manipulation of Maxwell's equations in a medium of finite conductivity yields the well-known differential equation

$$\nabla^2 \bar{E} = j\omega\mu_0(\sigma + j\omega\epsilon_0)\bar{E}, \tag{6}$$

where μ_0 and ϵ_0 are the free-space permeability and permittivity, respectively.

Under the assumption of piecewise constancy of the conductivity σ, Eq. (6) can be solved in conjunction with Eq. (5) yielding the following expressions for the attenuation α and phase shift β of the wave as it traverses the medium:

$$\alpha = \omega\sqrt{\mu_0\epsilon_0/2}\left\{-\left[1 - \omega_p^2/(\omega^2+\nu^2)\right] + \sqrt{\left[1 - \omega_p^2/(\omega^2+\nu^2)\right]^2 + (\nu^2/\omega^2)\left[\omega_p^2/(\omega^2+\nu^2)\right]^2}\right\}^{1/2}, \tag{7}$$

$$\beta = \omega\sqrt{\mu_0\epsilon_0/2}\left\{\left[1 - \omega_p^2/(\omega^2+\nu^2)\right] + \sqrt{\left[1 - \omega_p^2/(\omega^2+\nu^2)\right]^2 + (\nu^2/\omega^2)\left[\omega_p^2/(\omega^2+\nu^2)\right]^2}\right\}^{1/2}, \tag{8}$$

where ω_p, the electron plasma frequency, is defined as $\omega_p^2 = N_e e^2/\epsilon_0 m$.

Direct substitution of the N_e and ν profiles discussed earlier into Eqs. (7) and (8) gives values of attenuation and phase shift vs altitude. These curves are plotted in Figs. 5 through 10 for the three cases considered here, i.e., magnetically quiet ionosphere (twilight and night) and moderately disturbed ionosphere (twilight).

It is noteworthy at this point that the attenuation curves achieve a minimum in most instances at altitudes of interest and that this minimum is rather broad. Furthermore, the value of the attenuation at the minimum can be as low as $\approx 10^{-10}$ dB/m (for 30 MHz and quiet, nighttime conditions). For this extreme case of 10^{-10} dB/m one would expect a total attenuation of the wave per revolution around the earth of approximately 0.004 dB.

TRAPPING CONDITIONS AND THE M NUMBER

Low attenuation by itself is not enough to insure observable circulating signals. In order for the wave to circulate at constant altitude around the earth, the variations of the ionospheric properties in the immediate neighborhood of that altitude must be exactly right so as to impart to the wave a curvature equal to that of the earth's at each point of its trajectory. Obviously if that were not to happen, the wave would not circulate, and, in addition, its attenuation would be much higher since it would travel in regions of higher signal absorption.

Mathematically, this condition can be derived with the aid of Fig. 11.

Consider a spherical earth of radius a and a thin ionospheric layer of thickness dh at an altitude h above the earth's surface. Let two waves, one at altitude h and another at altitude $h + dh$, traverse an arc subtended by the angle ϕ centered at the earth's center.

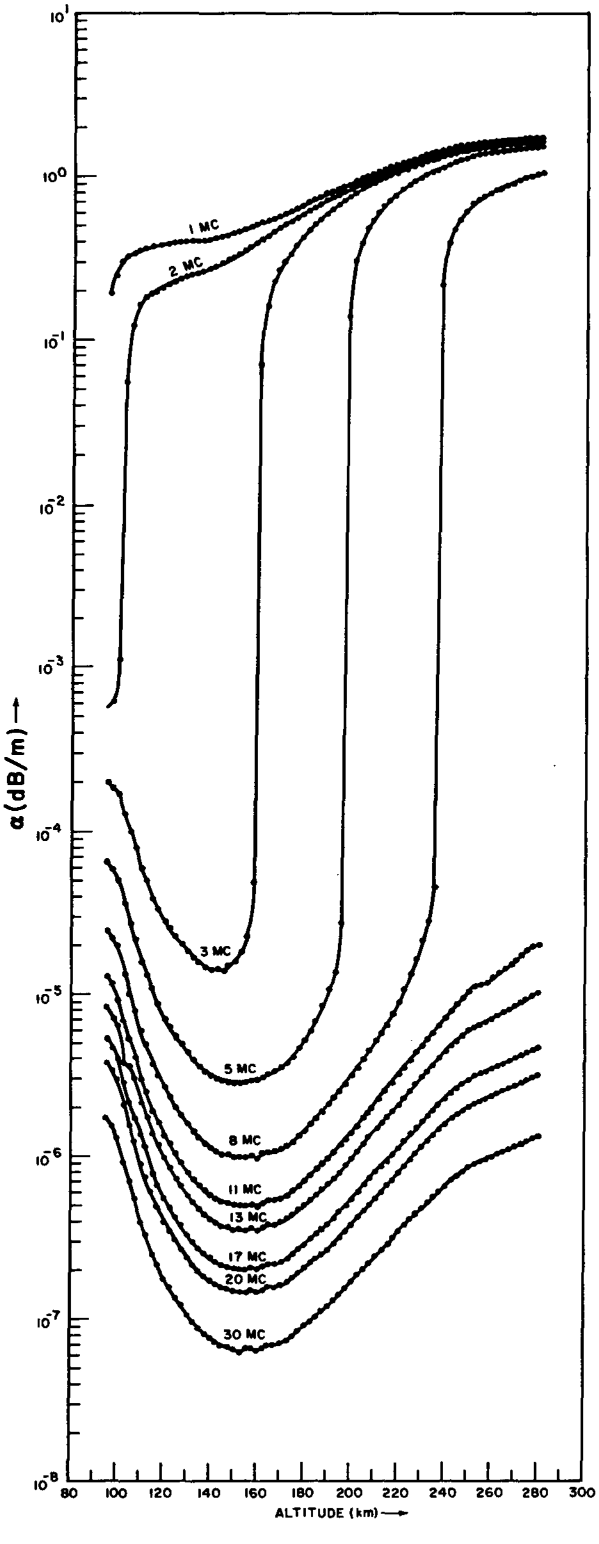

Fig. 5 - Attenuation profiles for magnetically quiet ionosphere — twilight

UNCLASSIFIED

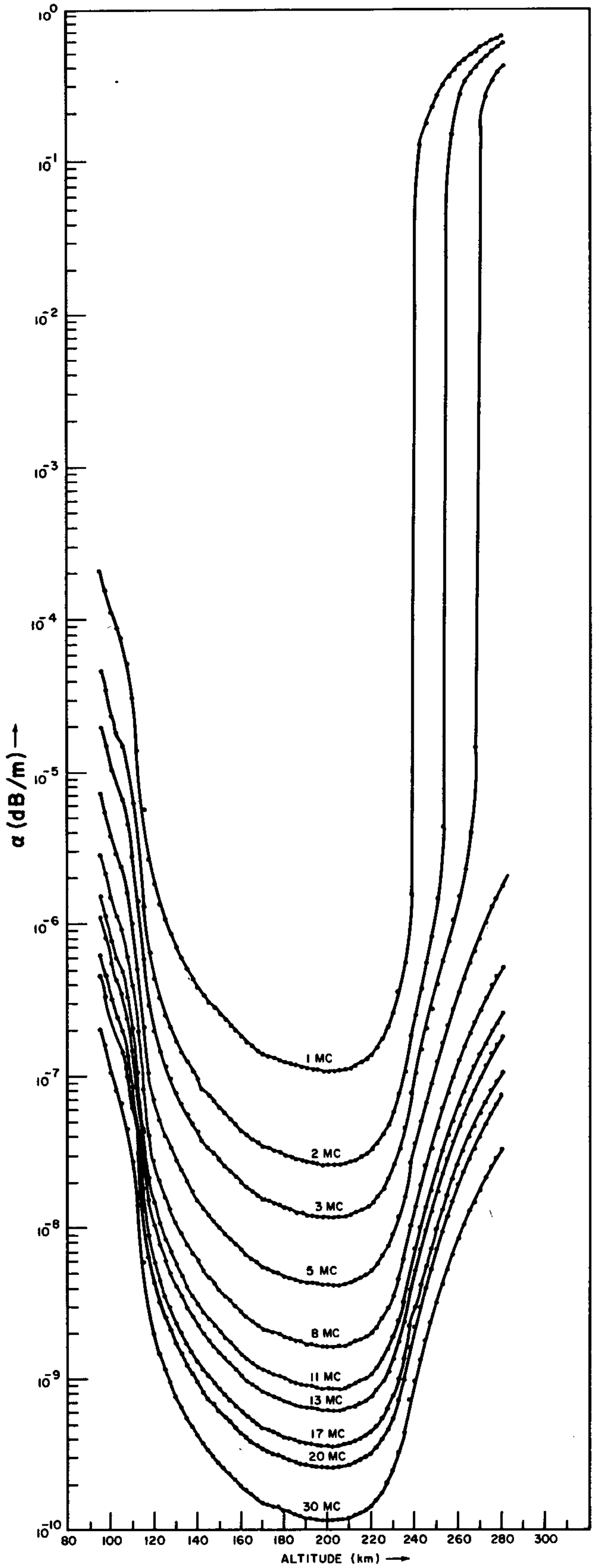

Fig. 6 - Attenuation profiles for magnetically quiet ionosphere — night

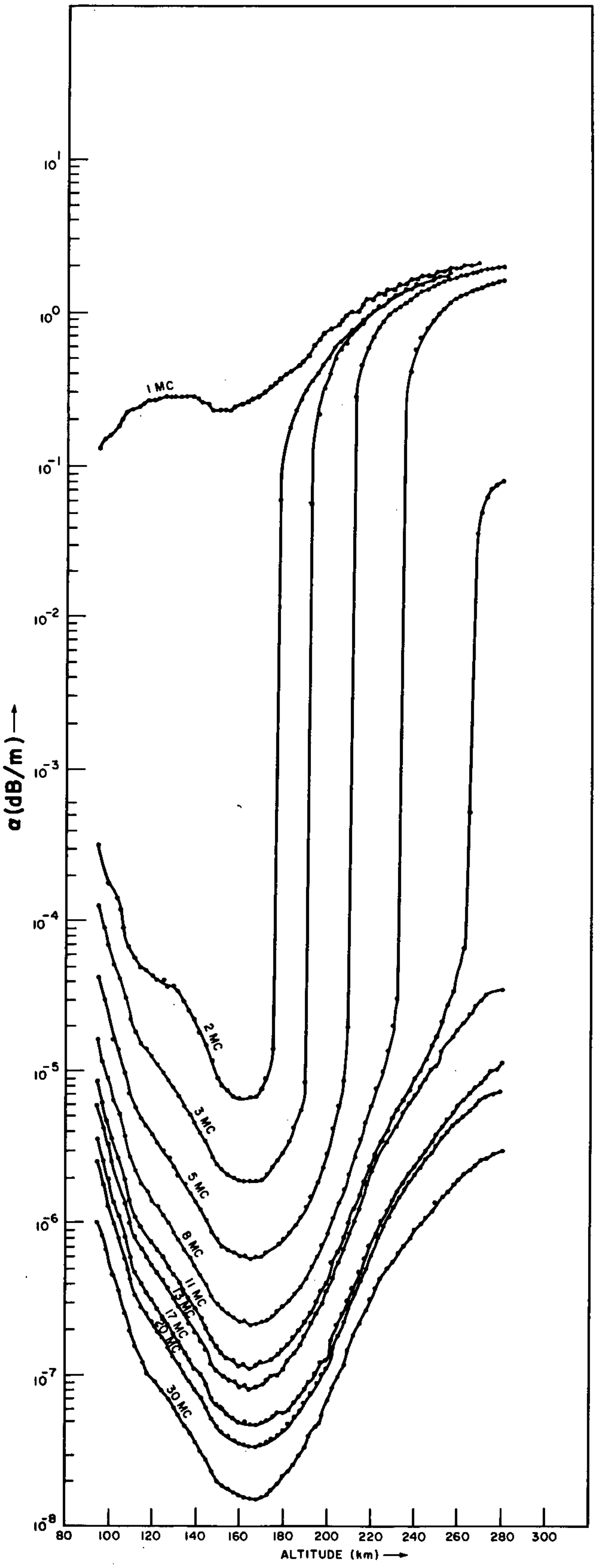

Fig. 7 - Attenuation profiles for moderately disturbed ionosphere — twilight

UNCLASSIFIED

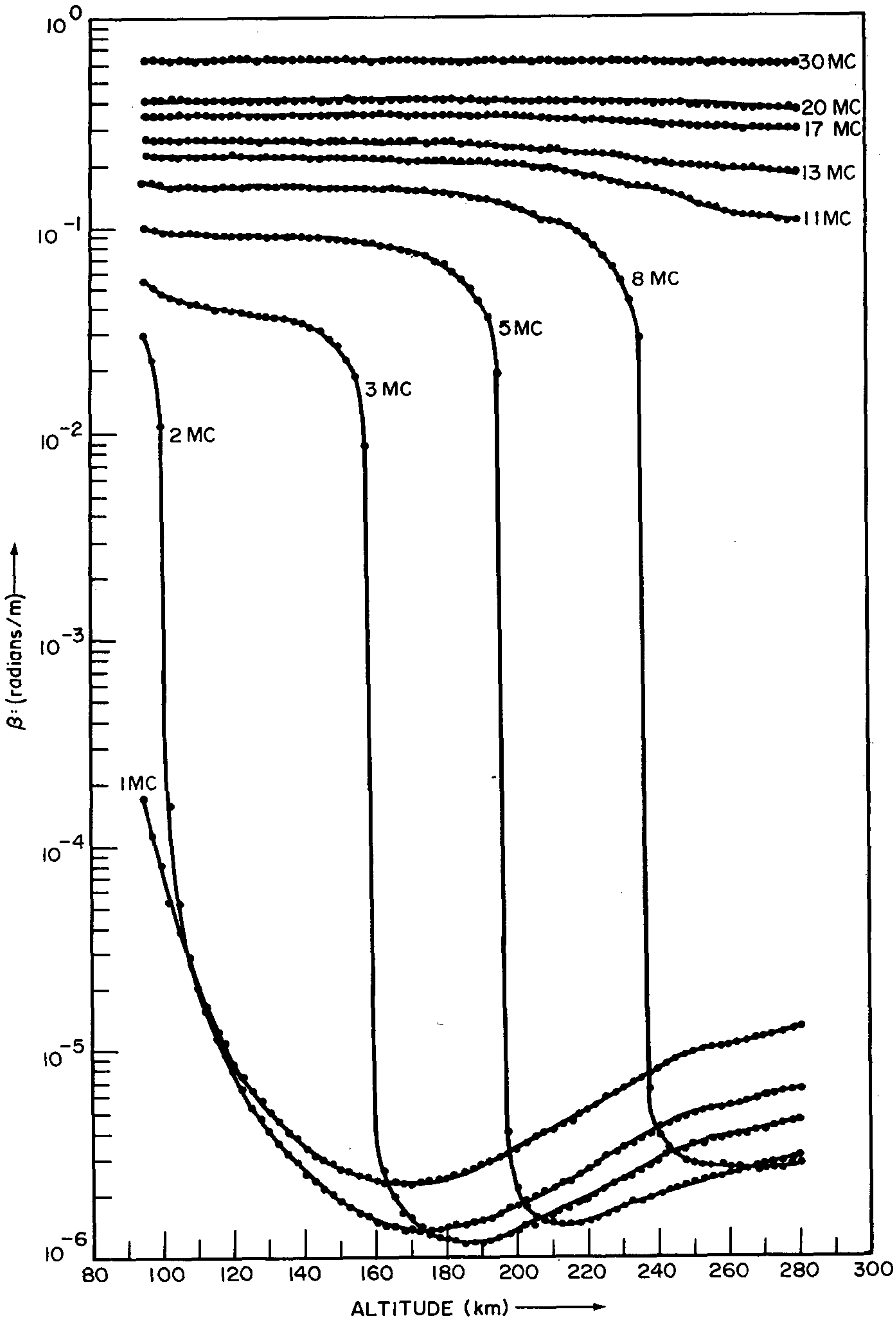

Fig. 8 - Phase shift profiles for magnetically quiet ionosphere — twilight

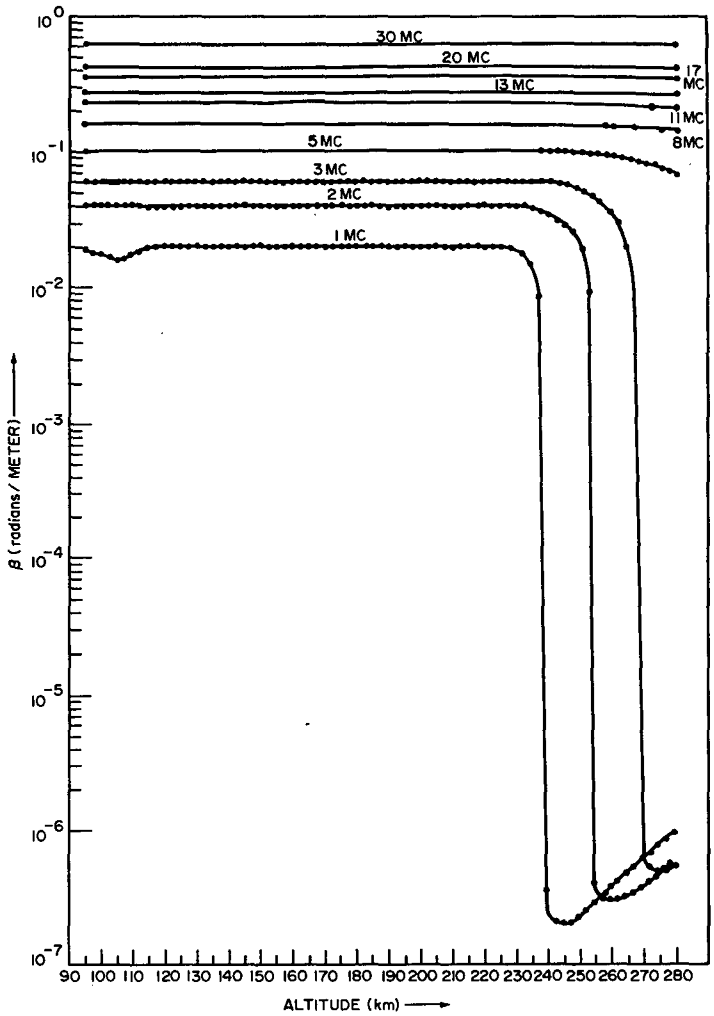

Fig. 9 - Phase shift profiles for magnetically quiet ionosphere — night

UNCLASSIFIED

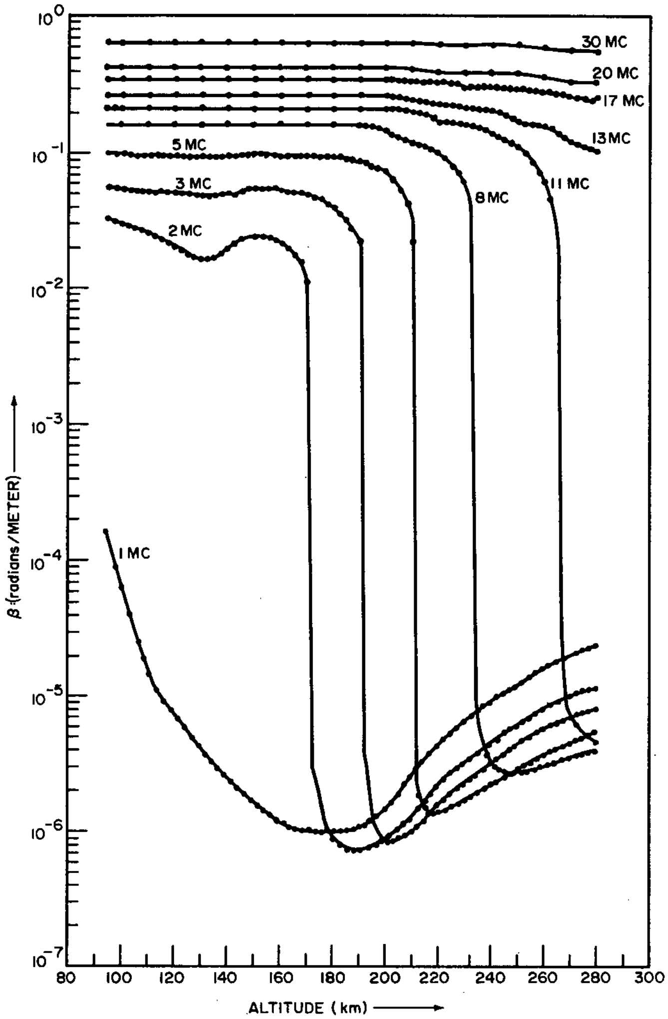

Fig. 10 - Phase shift profiles for moderately disturbed ionosphere — twilight

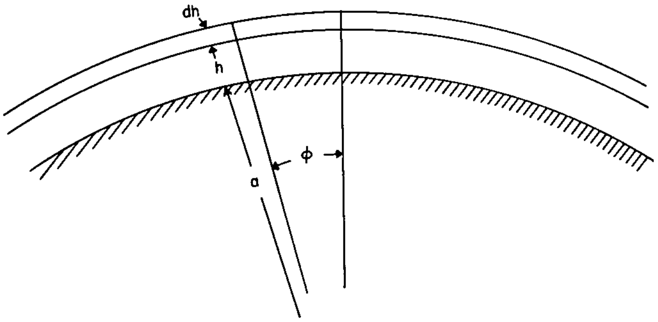

Fig. 11 - The trapping condition

The condition necessary for the two waves to travel the same angular distance about the earth, i.e., to bend with the same radius of curvature, is that the arcs which they both traverse be equal when expressed in wavelengths.

Mathematically this condition yields

$$\frac{\phi \cdot (a + h)}{\lambda(h)} = \frac{\phi \cdot (a + h + dh)}{\lambda(h + dh)}\,, \tag{9}$$

where $\lambda(h)$ is the wavelength at an altitude h. Thus,

$$\lambda(h) \cdot (a + h + dh) = \lambda(h + dh) \cdot (a + h)\,, \tag{10}$$

or

$$(a + h) \cdot \lambda(h) + \lambda(h)dh = (a + h) \cdot \left[\lambda(h) + \frac{d\lambda}{dh}\,dh\right], \tag{11}$$

which reduces to

$$\frac{d\lambda}{\lambda} = \frac{dh}{a + h}\,, \tag{12}$$

or

$$\frac{d\beta}{\beta} = -\frac{dh}{a + h}\,, \tag{13}$$

since the phase shift $\beta = 2\pi/\lambda$.

One could proceed to utilize the available β profiles and examine whether or not any of those profiles possess regions where Eq. (13) is satisfied. However, such a procedure would give a yes or no answer rather than the more complete description of the duct region desired here.

UNCLASSIFIED

The quantity known as the M number is introduced to simplify the presentation. The M number is a reduced refractive index and is used extensively in tropospheric refraction and superrefraction studies (8). Its use effectively changes the earth's curvature to infinity and thus "flattens" the earth. It is defined as

$$M(h) = \left[n(h) - \frac{a}{h + a}\right] 10^6 , \tag{14*}$$

where $n(h)$ is the refractive index. It is simply related to β by $n = \beta c/\omega$, c being the velocity of light. Note that the quantity $\beta = a/(h + a)$ is the solution of Eq. (13) with the boundary condition $\beta = 1$ when $h = 0$. Thus, condition (13) is equivalent to

$$\frac{d}{dh}\left[n(h) - \frac{a}{h + a}\right] = 0 \text{ or } \frac{dM}{dh} = 0. \tag{15}$$

Therefore, it is seen that points of maximum or minimum on M-vs-h curves correspond to points of ideal bending of electromagnetic waves for RTW propagation, provided of course that the waves are initially injected parallel to the earth's surface.

In a similar manner it can be shown that rays injected tangentially to the earth's surface will bend toward the earth if $dM/dh < 0$ and away from the earth if $dM/dh > 0$. Thus, points of M-number maximum are, in a sense, points of stable equilibrium since rays slightly above or below the altitude of maximum M will tend to converge toward that maximum and oscillate around it provided their angle does not exceed a critical angle ψ_{cr}. On the other hand, points where M attains a minimum can be called points of unstable equilibrium since rays slightly perturbed away from the minimum will always tend to diverge further from it, either toward the earth's surface or toward higher altitudes.

Al'pert (8) derives Eq. (16) for calculation of the trajectory of the rays given an M-number variation with height and an initial angle of injection into the region of interest:

$$r = \int \frac{dh}{\left[\psi_1^2 + 2(M - M_1)\, 10^{-6}\right]^{1/2}} \tag{16}$$

where r is the range along the earth's surface, ψ_1 is the injection angle at $h = h_1$, and M_1 is the M number at the same altitude. Equation (16) is an approximation and is good only for small values of ψ_1 ($\tan\psi_1 \approx \psi_1$) and subsequent angles between the ray path and the tangent to the earth's surface. Figure 12 is an example of the ray trajectories that result from parallel (to the earth's surface) injection at various altitudes for the case of quiet-twilight conditions and for a frequency of 20 MHz. The calculation was done as per Eq. (16) after linearization of the M-number profile.

RESULTS

With the above observations in mind, one can critically examine the M-number-vs-altitude curves for the three ionospheric conditions of interest. These curves are shown

*This definition is equivalent to the more usual form

$$M = \left[(n - 1) + \frac{h}{a}\right] 10^6$$

since for $h/a << 1$, $\frac{a}{h + a} \approx 1 - h/_a$.

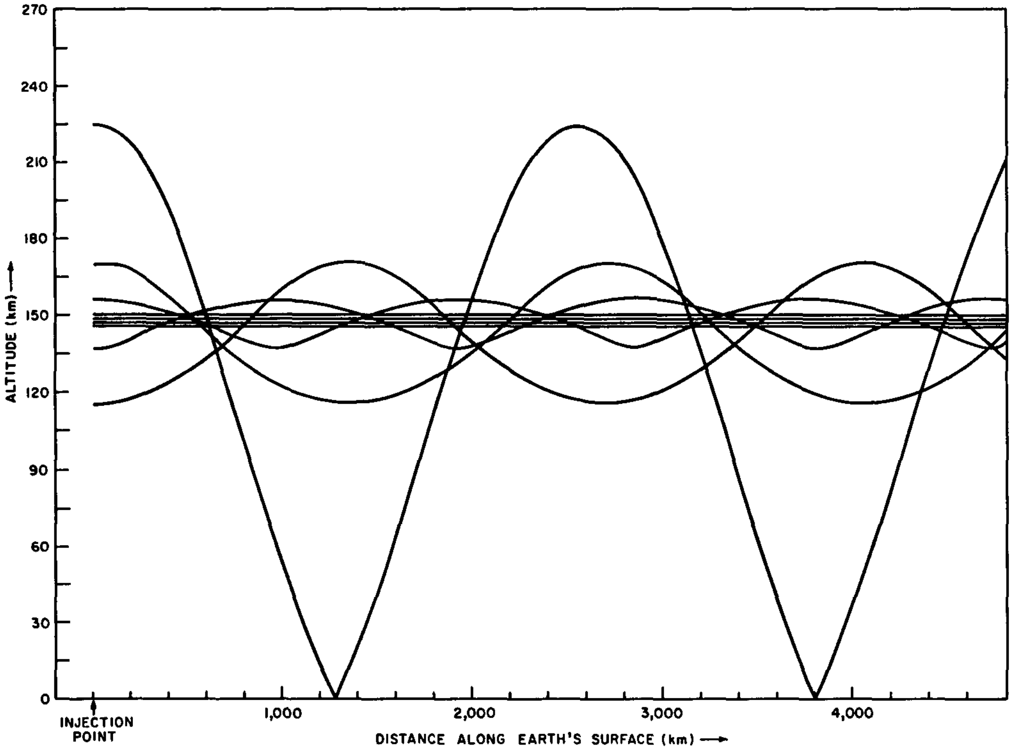

Fig. 12 - Calculated wave trajectories that result from parallel injection at various altitudes for the case of the quiet-twilight conditions and for a frequency of 20 MHz

in Figs. 13, 14, and 15. The waves follow the curvature of the earth wherever the solid lines are vertical ($\frac{dh}{dM} = \infty$). Superimposed on these profiles are attenuation curves (dashed curves), the attenuation being expressed in dB per 1000 km. Thus, given the electromagnetic frequency and the altitude of injection of a wave, the attenuation that it will suffer per 1000-km travel parallel to the earth's surface can be determined. Also, from the value of M at that point and the angle of injection the angle of refraction can be calculated over a path increment.

Table 1 summarizes some of the more interesting information extracted from Figs. 13 through 15. This table shows that a variety of conditions exists for which the total attenuation per revolution around the earth is less than 10 dB. For quiet-twilight and moderate-twilight conditions signals of frequencies greater than 15 MHz and 8 MHz, respectively, will suffer less than 10-dB attenuation in the ducted mode, while for nighttime conditions the total attenuation can be very small (i.e., probably less than 6 dB per revolution for all frequencies considered here). No detailed examination of echo delay times has been made. However, rough calculations indicate that when the reduced group velocity of the wave is taken into account, echo delay times for the ducted mode of propagation are about 138 milliseconds. This compares favorably with Al'pert's (8) quotation of an average delay time of 137.8 milliseconds for 785 RTW echo experiments over the same frequency range.

CONCLUSIONS

The work described in this report demonstrates that the properties of the ionosphere are such that RTW propagation can be achieved by (a) propagation within an elevated duct where the wave oscillates vertically between the duct boundaries or (b) propagation at, or

UNCLASSIFIED

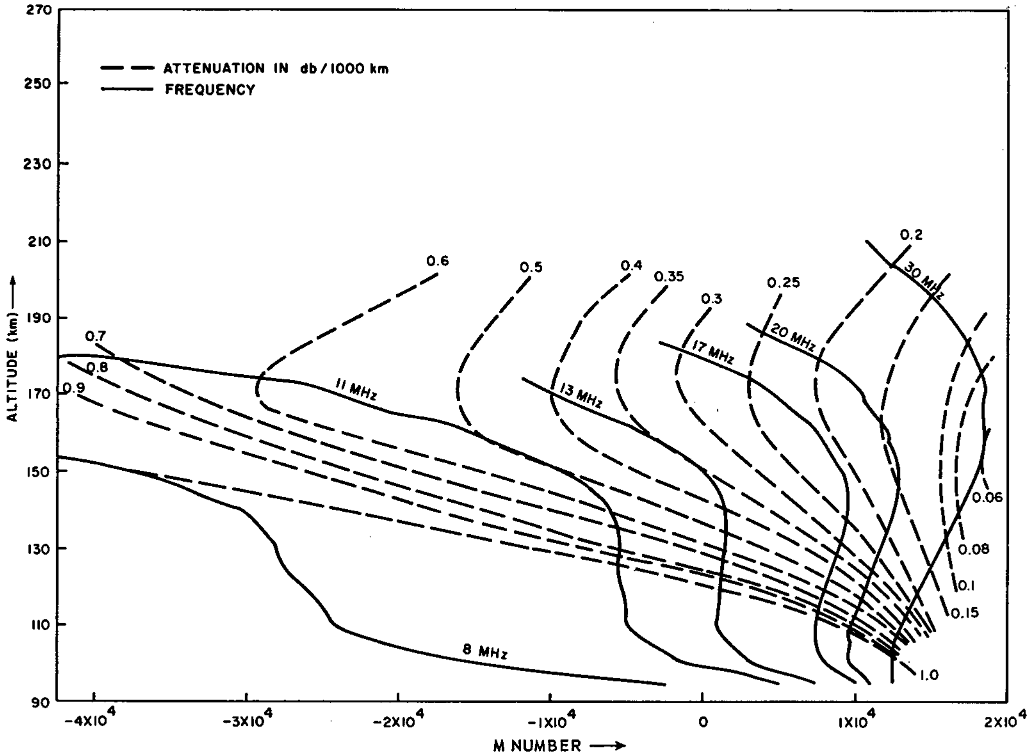

Fig. 13 - M-number profiles of magnetically quiet ionosphere — twilight

very near, the center of the duct where the wave glides practically at a constant radius of curvature along a path concentric with the earth's surface. A third mode, hop between the ionosphere and the earth's surface, is similarly explained, the mode depending on the injection angle and position. The mechanism for all three modes is identical and one can go smoothly from one to the other by changing the altitude and/or angle of injection or the electromagnetic frequency. A combination of two, or all three, of the modes is certainly not impossible provided appropriate "tilts" are present along the path length as Fenwick (9) suggests. From the point of view of attenuation, however, the second method, i.e., propagation at or near the center of the duct, seems the most promising.

Injection mechanisms not reported in this work play an important role in the interpretation of experimental data. Scattering in particular will add to the signal loss per unit path length.

Future work, it is felt, should consist mainly of experimentation, although there are theoretical aspects that are of interest (i.e., inclusion of static magnetic field, ray tracing from actual antenna patterns with the M-number profiles as a basis, etc.). Accurate echo delay time and attenuation measurements should be made by using transmitters and receivers on satellites whose orbits intersect the regions of interest. Satellite-satellite as well as satellite-ground links should be established to study not only the mode of propagation but also the injection mechanisms.

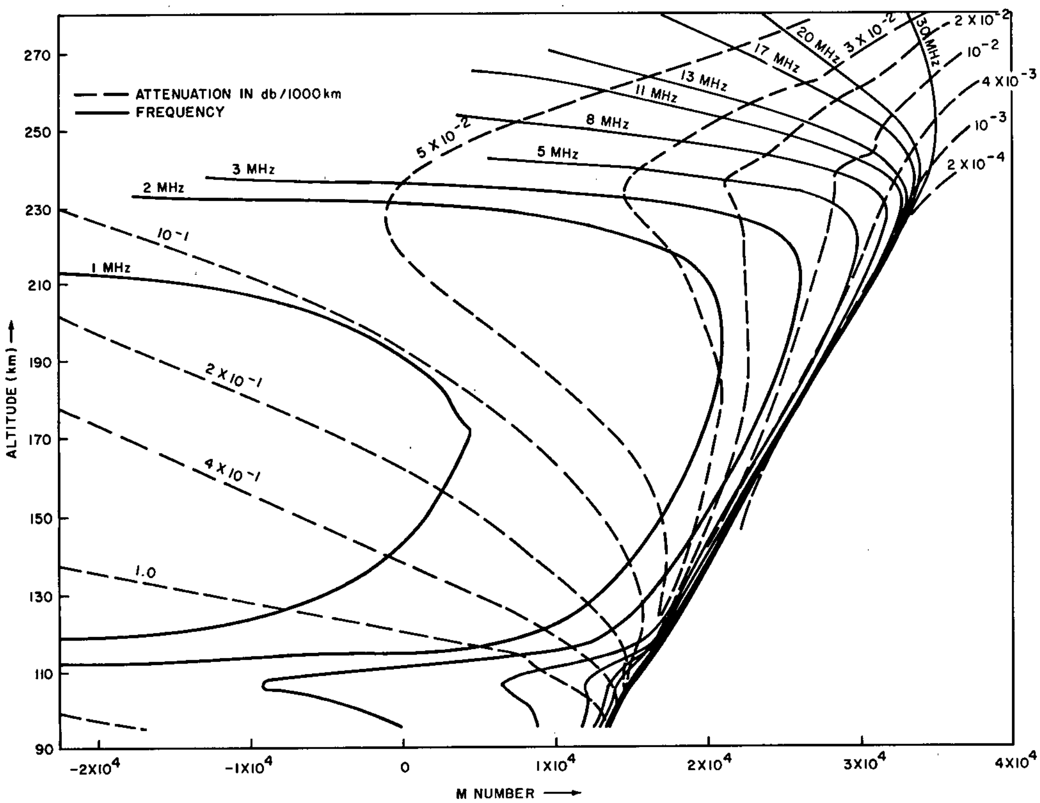

Fig. 14 - M-number profiles for magnetically quiet ionosphere — night

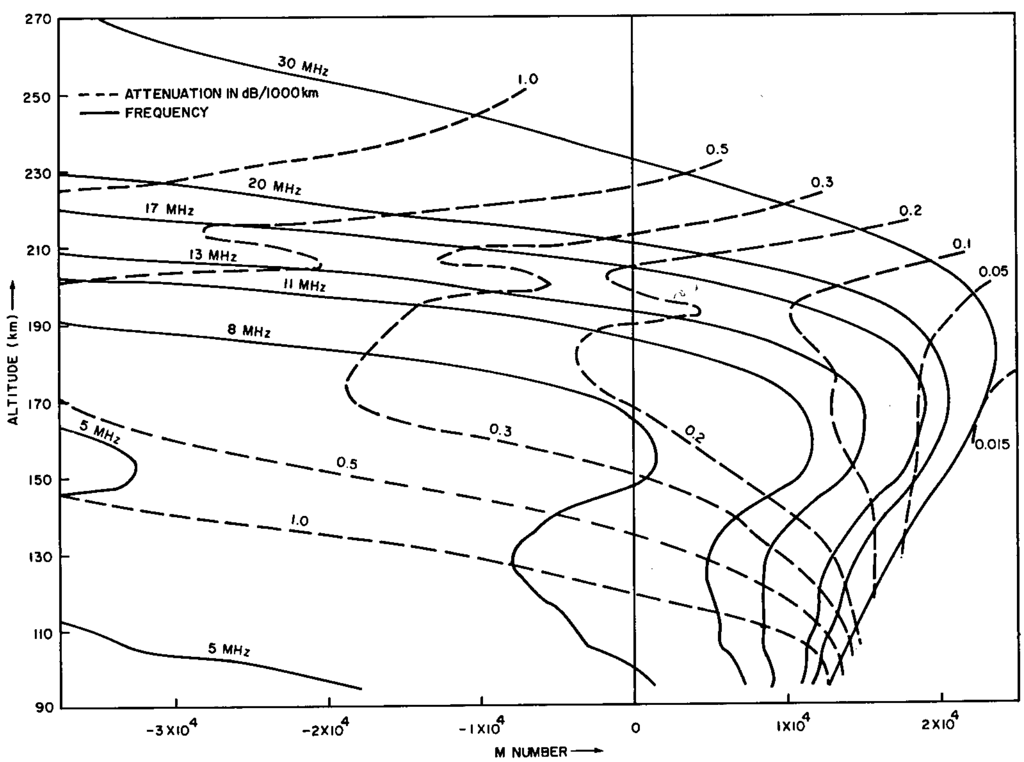

Fig. 15 - M-number profiles for moderately disturbed ionosphere — twilight

Table 1
Ionospheric Ducts and Their Properties

f (MHz)	Quiet Twilight		Quiet Night		Moderate Twilight	
	h(duct center) (km)	α(duct center) (dB/1000 km)	h(duct center) (km)	α(duct center) (dB/1000 km)	h(duct center) (km)	α(duct center) (dB/1000 km)
1	-	-	170	0.15	-	-
2	-	-	195	0.026	151	8.8
3	-	-	210	0.012	152	2.2
5	-	-	220	0.006	153	0.75
8	-	-	228	0.003	155	0.25
11	115 and 130	>0.8	232	0.002	154-165	0.12-0.15
13	130-140	0.4-0.6	234	0.0017	158-165	0.08
17	143	0.22	235	0.001	165-170	0.048
20	150	0.15	239	0.0015	173	0.035
30	160 and 172	0.06 and 0.07	250	0.003	185	0.025

UNCLASSIFIED

REFERENCES

1. Quäck, E., "Propagation of Short Waves Around the Earth," Proc. IRE:15:341-345 (1927)

2. Quäck, E., "Further Communication on the Propagation of Short-Waves," Proc. IRE 15:1065-1068 (1927)

3. Eckersley, T.L., "Short-Wave Wireless Telegraphy," J. IEE. 65:600-644 (1927)

4. Taylor, A.H., and Young, L.C., "Studies of High-Frequency Radio Wave Propagation," Proc. IRE 16:561-578 (1928)

5. Quäck, E., and Mogel, H., "Double and Multiple Signals with Short Waves," Proc. IRE 17:791-823 (1929)

6. Hess, H.A., "Investigations of High-Frequency Echoes," Proc. IRE 36:981-992 (1948)

7. Isted, G.A., "Round-the-World Echoes," Marconi Rev. 21:173-183 (1958)

8. Al'pert, Ya. L., "Radio Wave Propagation and the Ionosphere," Consultants Bureau Enterprises, Inc., 1963. (The Russian text was published by the USSR Academy of Sciences Press for the Institute of Terrestial Magnetism, the Ionosphere, and Propagation of Radio Waves in Moscow in 1960)

9. Whale, H.A., "Effects of Ionospheric Scattering on Very-Long-Distance Radio Communication," New York Plenum, 1969

10. Fenwick, R.B., "Round-the-World High-Frequency Propagation," Report SEL-63-019 (TR 71), Stanford University Electronics Laboratories, Stanford, Calif., Apr. 1963

11. Wakai, N., "Quiet and Disturbed Structure and Variations of the Nighttime E Region," J. of Geophys. Res. 72(No. 17):4507-4517 (1967)

12. Nicolet, M., "Collision Frequency of Electrons in the Terrestial Atmosphere," Phys. of Fluids 2(No. 2):95-99 (1959)

13. Minzner, R.A., Champion, K.S.W., and Pond, H.L., "The ARDC Model Atmosphere, 1959," Air Force Cambridge Research Center, Geophysics Research Directorate, Bedford, Mass., AFCRC-TR-59-267, Air Force Surveys in Geophysics, No. 115, 1959

14. Banks, P.M., "The Thermal Structure of the Ionosphere," Proc. IEEE 57 (No. 3): 258-281 (1969)

15. Banks, P., "Collision Frequencies and Energy Transfer-Electrons," Planetary and Space Sci. 14:1085-1103 (1966)

16. Colegrove, F.D., Johnson, F.S., and Hanson, W.B., "Atmospheric Composition in the Lower Thermosphere," J. of Geophys. Res. 71(No. 9):2227-2236 (1966)

UNCLASSIFIED

Security Classification

DOCUMENT CONTROL DATA - R & D

(Security classification of title, body of abstract and indexing annotation must be entered when the overall report is classified)

1. ORIGINATING ACTIVITY *(Corporate author)* Naval Research Laboratory Washington, D. C. 20390	2a. REPORT SECURITY CLASSIFICATION Unclassified
	2b. GROUP

3. REPORT TITLE

THE POSSIBILITY OF ELECTROMAGNETIC WAVE DUCTING IN THE IONOSPHERE

4. DESCRIPTIVE NOTES *(Type of report and inclusive dates)* This is a final report on the application of this study to the ionosphere; the study of inhomogeneous plasmas is continuing.

5. AUTHOR(S) *(First name, middle initial, last name)*

S.J. Stephanakis, W.W. Balwanz, W.S. Ament, and W.R. Faust

6. REPORT DATE	7a. TOTAL NO. OF PAGES	7b. NO. OF REFS
November 6, 1970	24	16

8a. CONTRACT OR GRANT NO. NRL Problem R07-07	9a. ORIGINATOR'S REPORT NUMBER(S) NRL Report 7171
b. PROJECT NO. RF 17-344-401-4503	
c.	9b. OTHER REPORT NO(S) *(Any other numbers that may be assigned this report)*
d.	

10. DISTRIBUTION STATEMENT

This document has been approved for public release and sale; its distribution is unlimited.

11. SUPPLEMENTARY NOTES	12. SPONSORING MILITARY ACTIVITY
	Department of the Navy (Office of Naval Research) Arlington, Virginia 22217

13. ABSTRACT

The refractive index of the ionosphere varies with altitude, providing optimum wave curvature for around-the-world propagation. The variation also provides ducts which tend to focus waves into this optimum curvature.

Simple calculations using published ionospheric properties are used to demonstrate the wave curvature and the duct structure. The duct altitude varies between 90 and 300 km depending on the frequencies used and the diurnal variations of the ionosphere. Signal loss varies widely, providing around-the-world propagation with less than a 5-dB loss per earth traverse in some of the duct configurations.

Methods of coupling into the ducts are assumed based on reports by other investigators. Signal scatter, which provides one method for coupling into and out of the duct, adds to the calculated signal loss from electron collisions.

DD FORM 1 NOV 65 1473 (PAGE 1)

S/N 0101-807-6801

Security Classification

Security Classification

14. KEY WORDS	LINK A		LINK B		LINK C	
	ROLE	WT	ROLE	WT	ROLE	WT
Ionosphere						
Attenuation profiles						
Phase shift profiles						
Ducting						
M number						
Trapping condition						
Electron density						
Collision frequency						
EM wave propagation						

DD FORM 1 NOV 65 1473 (BACK)
(PAGE 2)

Security Classification